Heliyon 10 (2024) e39394

Contents lists available at ScienceDirect

Heliyon

journal homepage: www.cell.com/heliyon

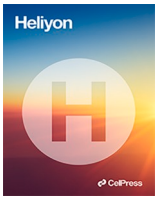

Research article

Insights into antibacterial design: Computational modeling of eugenol derivatives targeting DNA gyrase

Heba S. Elsewedy [a,*], Sultan Alshehri [b], Adeola T. Kola-Mustapha [c,d], Shaymaa M. Genedy [a], Khuzama M. Siddiq [a], Bushra Y. Asiri [a], Rehab A. Alshammari [a], Heba Mohammed Refat M. Selim [a,e], Oluwakorede J. Adedeji [d], George Oche Ambrose [f,**]

[a] Department of Pharmaceutical Sciences, College of Pharmacy, AlMaarefa University, P.O. Box 71666, Riyadh 11597, Saudi Arabia
[b] Department of Pharmaceutics, College of Pharmacy, King Saud University, Riyadh, 11451, Saudi Arabia
[c] Department of Pharmaceutics and Industrial Pharmacy, Faculty of Pharmaceutical Sciences, University of Ilorin, Ilorin, Nigeria
[d] College of Pharmacy, Alfaisal University Riyadh, Saudi Arabia
[e] Microbiology and Immunology Department, Faculty of Pharmacy (Girls), Al-Azhar University, Cairo 35527, Egypt
[f] University of Ilorin Teaching Hospital, Ilorin, Nigeria

ARTICLE INFO

Keywords:
Eugenol
DNA gyrase
Antibacterial
Molecular docking
Natural products

ABSTRACT

The rise of antibiotic resistance underscores the urgent need for novel antibacterial agents. DNA gyrase, an essential enzyme involved in bacterial DNA replication, is a promising target for antibacterial therapy. Computational approaches offer a cost-effective means to design and screen potential inhibitors, such as eugenol derivatives. This study aims to computationally design eugenol derivatives as potential antibacterial agents targeting DNA gyrase, assess their binding affinities, evaluate physicochemical properties, and toxicity, and select lead compounds for further investigation. Molecular docking simulations were conducted to investigate the binding affinities of eugenol derivatives and controls to DNA gyrase. Physicochemical properties and toxicity assessments of eugenol were evaluated. Lead compounds were selected based on drug likeness, toxicity, and binding affinity. Molecular docking studies revealed varying binding affinities of eugenol derivatives to DNA gyrase, with lead compounds exhibiting superior affinity compared to eugenol. Physicochemical properties indicated moderate lipophilicity and low aqueous solubility for eugenol. Toxicity assessment revealed mutagenicity and tumorigenicity. De novo compound synthesis generated 244 novel compounds, with 44 selected based on drug-likeness, toxicity, and binding affinity as lead candidates. These findings provide valuable insights for the development of novel antibacterial agents targeting DNA gyrase, with implications for combating antibiotic resistance.

1. Introduction

Eugenol, a naturally occurring phenolic compound, is widely recognized for its pharmacological properties and diverse biological activities. It is abundantly found in various plants, with cinnamon oil being one of its major natural sources [1]. Historically, eugenol

* Corresponding author.
** Corresponding author.
E-mail addresses: hsewedy@um.edu.sa (H.S. Elsewedy), Salshehri1@ksu.edu.sa (S. Alshehri).

https://doi.org/10.1016/j.heliyon.2024.e39394
Received 19 May 2024; Received in revised form 3 October 2024; Accepted 14 October 2024
Available online 19 October 2024

has been extensively utilized in traditional medicine for its analgesic, anti-inflammatory, antioxidant, and antimicrobial properties [1, 2]. Its broad spectrum of biological effects has garnered significant attention in biomedical research, particularly in the development of novel therapeutic agents against infectious diseases.

The emergence of antimicrobial resistance poses a critical challenge to public health globally, necessitating the exploration of alternative antimicrobial agents. DNA gyrase, a type II topoisomerase enzyme, plays a pivotal role in bacterial DNA replication and is an attractive target for antibacterial drug development [3]. In this context, eugenol and its derivatives have gained considerable interest due to their demonstrated antimicrobial activity against a wide range of bacterial pathogens, including both Gram-positive and Gram-negative bacteria [4]. However, the therapeutic efficacy of eugenol is hindered by its relatively lower binding affinity to DNA gyrase in comparison to established antibacterial agents like Isoquinoline Ethyl Ureas [5].

Cinnamon oil, a rich source of eugenol, offers a promising avenue for the development of eugenol-derived antibacterial agents. The unique chemical composition of cinnamon oil, characterized by a high eugenol content, provides a valuable starting point for computational drug design approaches aimed at enhancing the antibacterial activity of eugenol derivatives [6]. Computational methods, such as molecular docking and structure-based drug design, enable the rational design of novel compounds with improved pharmacological properties, including enhanced binding affinity and selectivity for specific molecular targets [7].

The application of computational techniques in drug design offers several advantages, including the ability to screen large compound libraries, predict binding interactions, and optimize molecular structures with desired pharmacokinetic properties [8]. By leveraging the evolutionary insights provided by molecular modeling tools and the extensive pharmacological knowledge of eugenol, researchers can systematically explore the chemical space surrounding eugenol to identify potential derivatives with superior

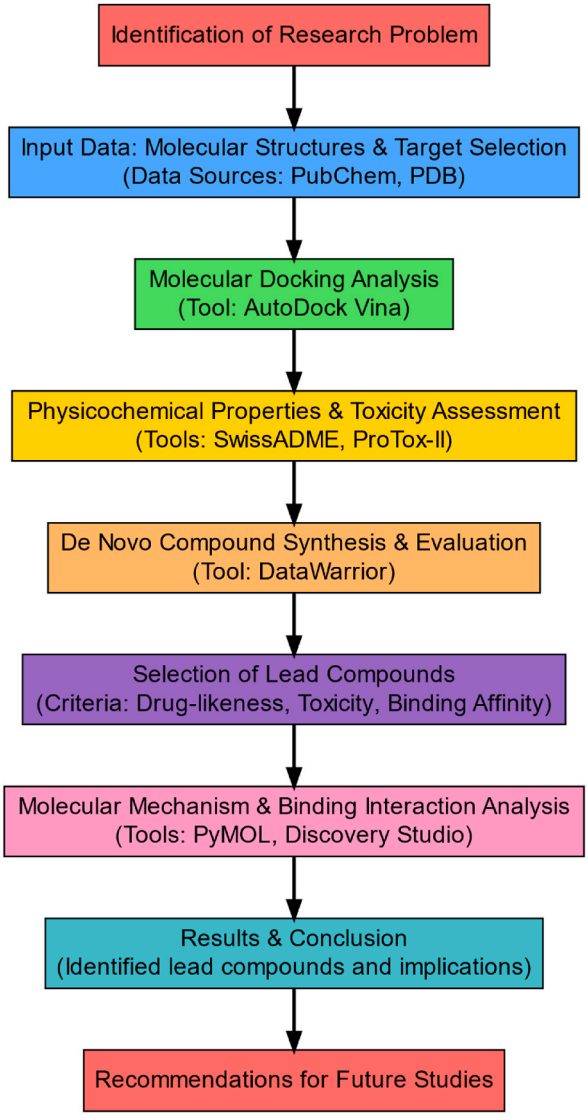

Fig. 1. Workflow for computational design of eugenol derivatives as antibacterial agents targeting DNA gyrase.

antibacterial activity against DNA gyrase [9].

In this study, we aim to harness the computational power of data-driven approaches to design eugenol derivatives as potential antibacterial agents targeting DNA gyrase. By integrating molecular docking simulations, structure-activity relationship analyses, and molecular dynamics simulations, we seek to elucidate the structural determinants governing the interaction between eugenol derivatives and DNA gyrase. Through rational computational design strategies, we endeavor to overcome the limitations of eugenol's inherent binding affinity and enhance its therapeutic potential as a promising antibacterial agent for combating drug-resistant bacterial infections.

2. Materials and methods

Fig. 1 illustrates the comprehensive workflow followed in this study for the computational design and evaluation of eugenol derivatives as potential antibacterial agents targeting DNA gyrase. The workflow begins with the identification of the research problem and selection of relevant molecular structures and target proteins. The input data, including molecular structures from databases such as PubChem and target selection for DNA gyrase, serves as the foundation for the study.

2.1. Molecular docking studies

Molecular docking analysis was performed using AutoDock Vina to explore the binding affinities of eugenol and Isoquinoline Ethyl Ureas to the DNA gyrase enzyme. The crystal structures of DNA gyrase with PDB IDs 5mmn, 5mmo, and 5mmp were obtained from the Protein Data Bank (PDB) and prepared for docking by removing water molecules and adding polar hydrogen atoms. The ligands, eugenol, and Isoquinoline Ethyl Ureas were retrieved from PubChem and prepared for docking by optimizing their 3D conformations and adding Gasteiger charges.

The grid box was centered at coordinates (x = 23.5234, y = 9.8694, z = 59.4146) with dimensions set to size_x = 25, size_y = 25, and size_z = 25, ensuring optimal coverage of the active site (Fig. S1; *Supplementary file*). The grid spacing was set to 0.375 Å, and a total of 10 docking runs were performed with an exhaustiveness setting of 8 to ensure comprehensive sampling of the docking space. The accuracy of docking predictions depends significantly on these parameters, making it crucial to define them explicitly in docking studies.

2.2. Binding affinities of eugenol and controls

The docking grids were defined to encompass the active sites of DNA gyrase as determined by the bound ligands in the crystal structures. Molecular docking was then performed with the prepared ligands against the DNA gyrase targets using AutoDock Vina, and the binding affinities were expressed in kcal/mol. The results were analyzed to compare the binding affinities of eugenol and Isoquinoline Ethyl Ureas to DNA gyrase across the three PDB IDs.

2.3. Physicochemical properties and toxicity assessment of eugenol

Physicochemical properties and toxicity measures of eugenol were evaluated to assess its drug-likeness and safety profiles. The molecular weight, partition coefficient (cLogP), aqueous solubility (cLogS), hydrogen bond acceptors (H-Acceptors), hydrogen bond donors (H-Donors), total surface area, relative polar surface area (PSA), and drug-likeness score were calculated using SwissADME. Additionally, toxicity assessments for mutagenicity, tumorigenicity, and reproductive effects were conducted using the ProTox-II server.

2.4. De novo compound synthesis and fitness evaluation

Novel compounds were generated from eugenol using the de novo compound generation tool in Datawarrior. A total of 244 compounds were synthesized, and their fitness for antibacterial activity targeting DNA gyrase was evaluated using a scoring function implemented in Datawarrior. The synthesis process was iterated through multiple generations to explore the chemical space around eugenol.

2.5. Selection of lead compounds

Lead compounds were selected based on stringent criteria, including drug-likeness assessment, toxicity evaluation, and molecular docking studies. Lipinski's rule of five was used as a primary filter for assessing drug-likeness properties, while toxicity profiles were evaluated for mutagenicity, tumorigenicity, and reproductive effects. Molecular docking studies were conducted to assess the binding affinity of selected compounds to DNA gyrase and compare them with eugenol.

2.6. Understanding molecular mechanisms

Detailed analyses of the binding interactions between the top hits and DNA gyrase were conducted to elucidate the molecular mechanisms underlying their enhanced binding affinity. The binding interactions were visualized and analyzed using PyMOL and

Discovery Studio Visualizer, focusing on hydrogen bonds, hydrophobic interactions, and electrostatic interactions. The localization of interacting residues within the Topo IIA-type catalytic domain was also investigated to understand their implications for the inhibitory effects of the top hits on DNA gyrase activity.

3. Results

3.1. Molecular docking studies

Molecular docking simulations were conducted to investigate the binding affinities of eugenol and Isoquinoline Ethyl Ureas to the DNA gyrase enzyme. The results are summarized in Tables 1–3, which present the binding affinities expressed in kcal/mol along with DNA gyrase with the corresponding PDB ID (5mmn, 5mmo, and 5mmp).

3.2. Binding affinities of eugenol and controls

Tables 1–3 display the binding affinities of eugenol and controls, Isoquinoline Ethyl Ureas, to the DNA gyrase enzyme across different PDB IDs. In Table 1, eugenol and a control compound exhibited varying binding affinities to the DNA gyrase enzyme (PDB ID: 5mmn). Eugenol showed a binding affinity of −45.067 kcal/mol, while the control compound demonstrated a higher binding affinity of −73.817 kcal/mol. Similarly, Table 2 presents the binding affinities of eugenol and another control compound to the DNA gyrase enzyme (PDB ID: 5mmo), with eugenol showing a binding affinity of −48.484 kcal/mol and the control compound exhibiting a significantly higher binding affinity of −80.793 kcal/mol. Table 3 illustrates the binding affinities of eugenol and a third control compound to the DNA gyrase enzyme (PDB ID: 5mmp), where eugenol demonstrated a binding affinity of −47.21 kcal/mol, while the control compound exhibited a notably higher binding affinity of −82.947 kcal/mol. The respective crystallographic information file's (CIF) report of the control ligands extracted from DNA gyrase (PDB ID: 5mmn, 5mmo and 5mmp) are contained in *Additional file 2*.

3.3. Physicochemical properties and toxicity assessment of eugenol

Physicochemical properties and toxicity measures of eugenol were evaluated to assess its drug-likeness and safety profiles. Tables 4 and 5 summarize the physicochemical properties and toxicity measures, respectively.

3.3.1. Physicochemical properties

Table 4 presents the physicochemical properties of eugenol, including molecular weight, partition coefficient (cLogP), aqueous solubility (cLogS), hydrogen bond acceptors (H-Acceptors), hydrogen bond donors (H-Donors), total surface area, relative polar surface area (PSA), and drug-likeness. The molecular weight of eugenol is about 164.203 KDa. The calculated partition coefficient (cLogP) value is 2.2723, indicating moderate lipophilicity. Aqueous solubility (cLogS) value is −2.05, suggesting low aqueous solubility for eugenol. Eugenol has hydrogen bond acceptors (2) and hydrogen bond donors (1). The total surface area is 140.17, and the polar surface area (PSA) is 29.46. Drug-likeness scores is −4.6405.

3.3.2. Toxicity measures

Table 5 provides toxicity measures for eugenol, including mutagenicity, tumorigenicity, and reproductive effects. Eugenol was assessed for their mutagenic and tumorigenic potential, with results indicating high mutagenicity and tumorigenicity. However, no reproductive effects was observed for the compound.

3.4. De novo compound synthesis and fitness evaluation

Novel compounds were synthesized using a de novo approach in Datawarrior to explore the chemical space around the parent compounds. A total of 244 novel compounds were generated from eugenol, and their fitness for antibacterial activity targeting DNA gyrase was evaluated. Fig. S2 (*Supplementary file*) summarizes the results of the synthesis process, including the parent generation, total count of synthesized compounds, mean value of fitness scores, standard deviation, and confidence interval (95 %). The scoring functions implemented in DataWarrior included parameters such as drug-likeness (based on Lipinski's rule of five), predicted toxicity profiles, and binding affinity scores [10]. Fitness scores were calculated as a weighted sum of these criteria, allowing us to rank compounds based on their potential as lead candidates [11]. The de novo compound generation approach leverages the chemical space surrounding the parent molecule to optimize for properties relevant to antibacterial efficacy [12].

Table 1
Comparison between the docking scores of Eugenol and 1-ethyl-3-[8-methyl-5-(2-methylpyridin-4-yl)isoquinolin-3-yl] urea.

Pubchem ID	Compounds	Binding affinity (kcal/mol) (PDB ID: 5mmn)
3314	Eugenol	−45.067
67448852	1-ethyl-3-[8-methyl-5-(2-methylpyridin-4-yl)isoquinolin-3-yl]urea	−73.817

Table 2
Comparison between the docking scores of Eugenol and prop-2-ynyl ~ {N}-[[3-(ethylcarbamoylamino)-5-pyridin-4-yl-isoquinolin-8-yl]methyl] carbamate.

Pubchem ID	Compounds	Binding affinity (kcal/mol) (PDB ID: 5mmo)
3314	Eugenol	−48.484
62705044	prop-2-ynyl ~ {N}-[[3-(ethylcarbamoylamino)-5-pyridin-4-yl-isoquinolin-8-yl]methyl] carbamate	−80.793

Table 3
Comparison between the docking scores of Eugenol and 1-ethyl-3-[5-pyridin-4-yl-8-(pyridin-3-ylamino)isoquinolin-3-yl]urea.

Pubchem ID	Compounds	Binding affinity (kcal/mol) (PDB ID: 5mmp)
3314	Eugenol	−47.21
67450369	1-ethyl-3-[5-pyridin-4-yl-8-(pyridin-3-ylamino)isoquinolin-3-yl]urea	−82.947

Table 4
Physicochemical properties of eugenol.

Physicochemical properties	values
Molweight	164.203 KDa
cLogP	2.2723
cLogS	−2.05
H-Acceptors	2
H-Donors	1
Total Surface Area	140.17
Relative PSA	0.1648
Polar Surface Area	29.46
Druglikeness	−4.6405

Table 5
Toxicity assessment of eugenol.

Toxicity	Measures
Mutagenic	high
Tumorigenic	high
Reproductive Effective	none

3.4.1. Parent generation and synthesized compounds

The parent generation indicates the iteration number of the synthesis process, with higher generations representing subsequent rounds of compound generation. A total of 12 compounds were synthesized in the initial generation (Generation 0), with the number of compounds increasing in subsequent generations, reaching a maximum of 63 compounds in Generation 2. The number of synthesized compounds gradually decreased in later generations, with only 4 compounds generated in Generation 7.

3.4.2. Fitness evaluation

The fitness of each synthesized compound was evaluated based on predetermined criteria, reflecting their potential as antibacterial agents targeting DNA gyrase. The mean value of fitness scores ranged from 0.85406 to 0.91197 across different generations. The standard deviation of fitness scores provides insight into the variability of fitness values within each generation, with lower values indicating less variability. Confidence intervals (95 %) were calculated to estimate the range within which the true population mean of fitness scores is likely to fall.

3.5. Selection of lead compounds

From the pool of 244 novel compounds synthesized through de novo compound generation, a rigorous selection process was employed to identify lead compounds with desirable drug-like properties, favorable binding affinity to DNA gyrase, and minimal toxicity concerns *(Additional file 1)*. Among these criteria, Lipinski's rule of five was used as a primary filter to assess drug-likeness properties.

Of the 244 novel compounds, only 44 passed Lipinski's rule of five, indicating favorable physicochemical properties conducive to oral bioavailability and pharmacokinetic properties suitable for drug development. These compounds exhibited appropriate molecular weight, lipophilicity (cLogP), aqueous solubility (cLogS), hydrogen bond acceptors, and donors within the acceptable ranges specified by Lipinski's criteria.

Furthermore, the toxicity profiles of the 44 selected compounds were assessed based on mutagenicity, tumorigenicity, and reproductive effects. None of these compounds exhibited high mutagenic or tumorigenic potential, and they were deemed safe for further investigation based on these toxicity parameters.

In addition to drug-likeness and toxicity evaluation, the binding affinity of the 44 selected compounds to DNA gyrase was assessed using molecular docking studies. These compounds demonstrated superior binding affinity to DNA gyrase compared to eugenol, the parent compound. The enhanced binding affinity of these compounds suggests their potential as effective inhibitors of DNA gyrase, a promising target for antibacterial therapy.

Based on the stringent criteria outlined above, a subset of 44 novel compounds emerged as promising lead candidates for further preclinical evaluation and drug development efforts. These compounds possess desirable drug-like properties, minimal toxicity concerns, and superior binding affinity to DNA gyrase, highlighting their potential as novel antibacterial agents for combating bacterial infections.

3.6. Understanding molecular mechanisms

To gain insights into the molecular mechanisms underlying the increased binding affinity between the top hits and their respective targets, detailed analyses of the binding interactions were conducted. Compound 24 from Table S1 *(Additional file 2)* emerged as the top hit for DNA gyrase (PDB ID: 5mmn).

3.6.1. Binding interactions of compound 24 with DNA gyrase

The binding interactions of Compound 24 with DNA gyrase were characterized by a series of hydrogen bonds, hydrophobic interactions, and electrostatic interactions. Notably, Compound 24 formed conventional hydrogen bonds with the side chain of GLU50, as evidenced by interactions between the nitrogen atom of Compound 24 and the oxygen atom of GLU50 (distance: 2.90543 Å). Additionally, carbon hydrogen bonds were observed between the carbon atom of Compound 24 and the oxygen atom of GLU50 (distance: 3.69981 Å) (Table 6; Fig. 2a, b, c). The hydrogen bond with GLU50 is significant because this residue plays a critical role in stabilizing the DNA-enzyme complex [13]. Inhibitors targeting this residue, such as fluoroquinolones, trap DNA gyrase in a cleavage complex, preventing the re-ligation of DNA strands and leading to bacterial cell death [14]. The observed interaction suggests that Compound 24 could function through a similar mechanism, highlighting its potential as an effective DNA gyrase inhibitor [15].

Furthermore, Compound 24 engaged in electrostatic interactions with GLU50, forming a pi-anion interaction. Hydrophobic interactions were also prominent, with Compound 24 interacting with various residues such as ILE78, VAL43, and VAL167 through alkyl interactions (Table 6).

3.6.2. Binding interactions of control compound with DNA gyrase

In comparison, the control compound (**1-ethyl-3-[8-methyl-5-(2-methylpyridin-4-yl)isoquinolin-3-yl] urea**) displayed a distinct set of binding interactions with DNA gyrase. Conventional hydrogen bonds were observed between the control compound and residues ASN46 and VAL43, indicative of favorable interactions contributing to binding affinity. Hydrophobic interactions, including amide-pi stacked interactions, were also noted between the control compound and residues such as GLY77, ILE78, and PRO79 (Table 7; Fig. 3a, b, c).

3.6.3. Comparison of binding interactions

Comparison of the binding interactions between Compound 24 and the control compound (**1-ethyl-3-[8-methyl-5-(2-methylpyridin-4-yl)isoquinolin-3-yl] urea**) revealed differences in the nature and extent of interactions with DNA gyrase. Compound 24 exhibited a higher number of hydrogen bonds and a more diverse array of hydrophobic interactions compared to the control compound, suggesting a stronger and more stable binding interaction.

To elucidate the molecular mechanisms underlying the enhanced binding affinity between the top hits and their respective targets, detailed analyses of the binding interactions were conducted. Compound 1 from Table S1 *(Additional file 1)* emerged as the top hit for DNA gyrase (PDB ID: 5mmp)

Table 6
Chemical interactions of Compound 24 within the binding pocket of DNA gyrase.

Name	XYZ:X	XYZ:Y	XYZ:Z	Distance	Category	Types
N:UNK1:H - A:GLU50:OE1	−48.7955	−0.108	0.874	2.90543	Hydrogen Bond	Conventional Hydrogen Bond
N:UNK1:C - A:GLU50:OE1	−48.694	−0.558	2.2955	3.69981	Hydrogen Bond	Carbon Hydrogen Bond
A:GLU50:OE1 - N:UNK1	−47.8042	0.965667	1.671	4.17496	Electrostatic	Pi-Anion
A:ASN46:C,O;ALA47:N - N:UNK1	−45.654	2.27333	3.6755	5.39239	Hydrophobic	Amide-Pi Stacked
N:UNK1 - A:ILE78	−47.9982	5.81412	4.29271	5.09007	Hydrophobic	Alkyl
N:UNK1:C - A:VAL43	−42.4932	7.98583	6.08767	5.05261	Hydrophobic	Alkyl
N:UNK1:C - A:VAL167	−43.9367	9.30067	4.96567	4.41741	Hydrophobic	Alkyl
N:UNK1:C - A:VAL43	−42.9522	7.73783	7.55617	4.24933	Hydrophobic	Alkyl
N:UNK1:C - A:VAL120	−45.4047	7.41317	8.89317	4.15566	Hydrophobic	Alkyl
N:UNK1:C - A:VAL167	−44.3957	9.05267	6.43417	4.74667	Hydrophobic	Alkyl
N:UNK1 - A:ILE78	−49.23	4.63529	3.24788	4.55216	Hydrophobic	Pi-Alkyl

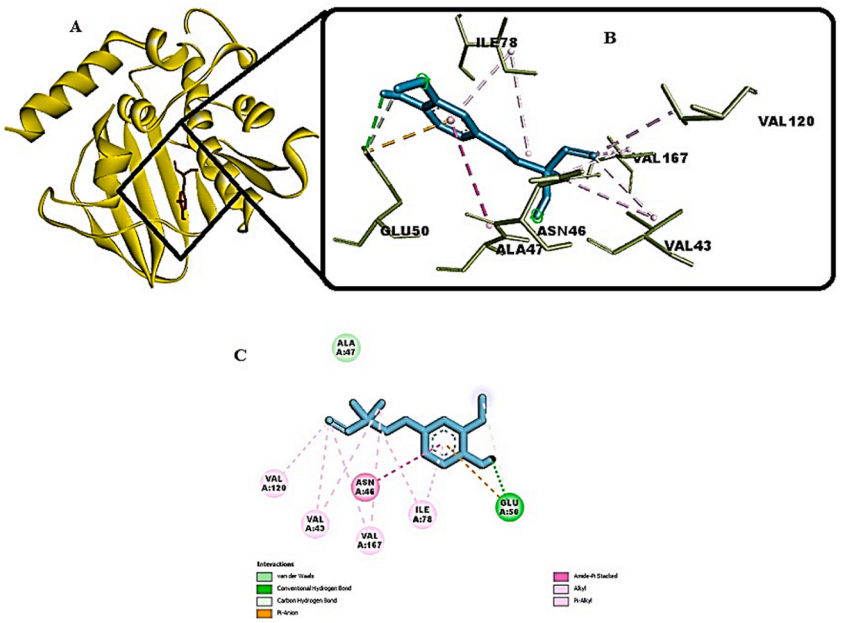

Fig. 2. (a) Compound 24 within the binding pocket of DNA gyrase (5MMN) (b) 2D and (c) 3D chemical interactions of compound 24 within the druggable pocket of DNA gyrase (5MMN).

Table 7
Chemical interactions of **1-ethyl-3-[8-methyl-5-(2-methylpyridin-4-yl)isoquinolin-3-yl] urea** within the binding pocket of DNA gyrase.

Name	XYZ:X	XYZ:Y	XYZ:Z	Distance	Category	Types
A:ASN46:HD22 - N:UNK1:O	−46.7095	1.0105	8.8535	2.86105	Hydrogen Bond	Conventional Hydrogen Bond
N:UNK1:HN - A:VAL43:O	−42.177	6.269	6.2945	2.80361	Hydrogen Bond	Conventional Hydrogen Bond
A:ASN46:C,O;ALA47:N - N:UNK1	−45.5507	2.44308	4.05533	5.00954	Hydrophobic	Amide-Pi Stacked
A:GLY77:C,O;ILE78:N - N:UNK1	−49.401	4.01775	1.66733	4.7916	Hydrophobic	Amide-Pi Stacked
N:UNK1:C - A:PRO79	−52.3373	2.415	2.30533	5.41368	Hydrophobic	Alkyl
N:UNK1:C - A:VAL43	−43.1237	7.93333	7.72617	4.32587	Hydrophobic	Alkyl
N:UNK1:C - A:VAL120	−45.5762	7.60867	9.06317	3.64012	Hydrophobic	Alkyl
N:UNK1:C - A:VAL167	−44.5672	9.24817	6.60417	4.54711	Hydrophobic	Alkyl
N:UNK1 - A:ILE78	−49.1267	4.80504	3.62771	4.21755	Hydrophobic	Pi-Alkyl

3.6.4. Binding interactions of compound 1 with DNA gyrase

The binding interactions of Compound 1 with DNA gyrase exhibited a diverse array of interactions, including hydrogen bonds, electrostatic interactions, and hydrophobic interactions. Notably, Compound 1 formed conventional hydrogen bonds with the side chain of GLU50, as evidenced by interactions between the hydrogen atom of Compound 1 and the oxygen atom of GLU50 (distance: 2.58634 Å) (Table 8; Fig. 4a, b, c).

Additionally, Compound 1 engaged in electrostatic interactions with GLU50, forming a pi-anion interaction. Hydrophobic interactions were also observed, with Compound 1 interacting with various residues such as ALA47, ILE78, VAL43, VAL120, VAL167, and VAL71 through alkyl interactions (Table 8; Fig. 4a, b, c).

3.6.5. Binding interactions of control compound with DNA gyrase

In contrast, the control compound exhibited distinct binding interactions with DNA gyrase. Conventional hydrogen bonds were observed between the control compound (**1-ethyl-3-[5-pyridin-4-yl-8-(pyridin-3-ylamino)isoquinolin-3-yl] urea**) and residues ASN46 and THR165, indicative of favorable interactions contributing to binding affinity. Hydrophobic interactions, including pi-sigma interactions and amide-pi stacked interactions, were also noted between the control compound and residues such as ALA47, VAL167, and ILE78 (Table 9; Fig. 5a, b, c).

3.6.6. Comparison of binding interactions

Comparison of the binding interactions between Compound 1 and the control compound (**1-ethyl-3-[5-pyridin-4-yl-8-(pyridin-3-ylamino)isoquinolin-3-yl] urea**) revealed differences in the nature and extent of interactions with DNA gyrase. Compound 1 displayed a higher number of hydrogen bonds and a more diverse array of hydrophobic interactions compared to the control compound, suggesting a stronger and more stable binding interaction.

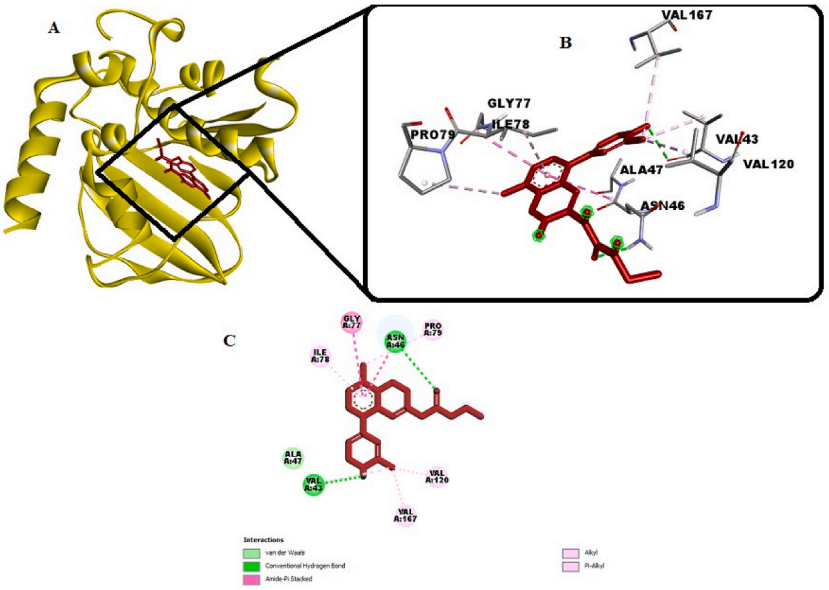

Fig. 3. (a) 1-ethyl-3-[8-methyl-5-(2-methylpyridin-4-yl)isoquinolin-3-yl]urea within the binding pocket of DNA gyrase (5MMN) (b) 2D and (c) 3D chemical interactions of **1-ethyl-3-[8-methyl-5-(2-methylpyridin-4-yl)isoquinolin-3-yl] urea** within the druggable pocket of DNA gyrase (5MMN).

Table 8
Chemical interactions of Compound 1 within the binding pocket of DNA gyrase.

Name	XYZ:X	XYZ:Y	XYZ:Z	Distance	Category	Types
N:UNK1:H - A:GLU50:OE1	48.0785	−19.492	−15.7505	2.58634	Hydrogen Bond	Conventional Hydrogen Bond
A:GLU50:OE1 - N:UNK1	47.9343	−18.8429	−14.2305	3.93396	Electrostatic	Pi-Anion
A:ALA47 - N:UNK1:C	50.159	−14.2465	−9.013	3.91904	Hydrophobic	Alkyl
N:UNK1 - A:ILE78	44.5017	−15.7899	−11.4064	5.34762	Hydrophobic	Alkyl
N:UNK1:C - A:VAL43	45.9203	−14.389	−5.655	4.32962	Hydrophobic	Alkyl
N:UNK1:C - A:VAL120	43.7405	−15.9658	−6.47717	4.27158	Hydrophobic	Alkyl
N:UNK1:C - A:VAL167	44.8037	−13.1968	−7.20717	4.27889	Hydrophobic	Alkyl
N:UNK1:C - A:VAL71	49.4602	−12.0438	−7.27217	4.44341	Hydrophobic	Alkyl
N:UNK1 - A:ILE78	44.6053	−16.6627	−13.1829	4.70435	Hydrophobic	Pi-Alkyl

Compound 1, identified as the top hit for DNA gyrase (PDB ID: 5mmo) from Table S1 *(Additional file 1)*, was compared with the control compound against the same target.

3.6.7. Binding interactions of compound 1 with DNA gyrase

The binding interactions of Compound 1 with DNA gyrase revealed a range of interactions contributing to its binding affinity. Conventional hydrogen bonds were observed between Compound 1 and residues GLY77 and GLU50, indicative of favorable interactions. Additionally, Compound 1 engaged in carbon hydrogen bonds with GLU50 and formed electrostatic interactions, specifically pi-anion interactions, with the same residue. Hydrophobic interactions were evident, with Compound 1 interacting with residues such as ALA47, ILE78, VAL43, VAL120, VAL167, and VAL71 through alkyl interactions (Table 10; Fig. 6a, b, c).

3.6.8. Binding interactions of control compound with DNA gyrase

In contrast, the control compound exhibited distinct binding interactions with DNA gyrase. Conventional hydrogen bonds were formed between the control compound (**prop-2-ynyl ∼ {N}-[[3-(ethylcarbamoylamino)-5-pyridin-4-yl-isoquinolin-8-yl] methyl] carbamate**) and residues ASN46, ARG76, GLU50, and VAL43, indicating favorable interactions contributing to binding affinity. Furthermore, hydrophobic interactions, including amide-pi stacked interactions and pi-alkyl interactions, were observed between the control compound (**prop-2-ynyl ∼ {N}-[[3-(ethylcarbamoylamino)-5-pyridin-4-yl-isoquinolin-8-yl] methyl] carbamate**) and residues such as ALA47 and ILE78 (Table 11; Fig. 7a, b, c).

3.6.9. Comparison of binding interactions

Comparison of the binding interactions between Compound 1 and the control compound (**prop-2-ynyl ∼{N}-[[3-(ethylcarbamoylamino)-5-pyridin-4-yl-isoquinolin-8-yl] methyl] carbamate**) revealed differences in the nature and extent of

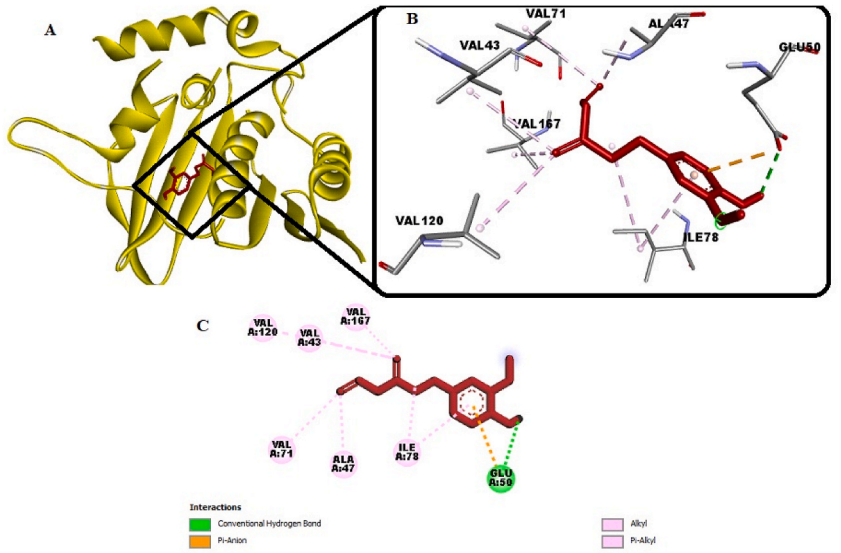

Fig. 4. (a) Compound 1 within the binding pocket of DNA gyrase (5MMP) (b) 2D and (c) 3D chemical interactions of compound 1 within the druggable pocket of DNA gyrase (5MMP).

Table 9
Chemical interactions of 1-ethyl-3-[5-pyridin-4-yl-8-(pyridin-3-ylamino)isoquinolin-3-yl]urea within the binding pocket of DNA gyrase.

Name	XYZ:X	XYZ:Y	XYZ:Z	Distance	Category	Types
A:ASN46:HD21 - N:UNK1:O	44.383	−21.8015	−7.02	2.84233	Hydrogen Bond	Conventional Hydrogen Bond
A:THR165:CG2 - N:UNK1	45.9598	−14.0724	−10.5296	3.9299	Hydrophobic	Pi-Sigma
A:ASN46:C,O;ALA47:N - N:UNK1	47.8216	−18.5888	−10.4554	4.61998	Hydrophobic	Amide-Pi Stacked
N:UNK1 - A:ALA47	48.9433	−15.5454	−8.93358	4.96223	Hydrophobic	Pi-Alkyl
N:UNK1 - A:VAL167	45.341	−13.2707	−7.98375	5.29469	Hydrophobic	Pi-Alkyl
N:UNK1 - A:ILE78	44.3009	−17.1335	−12.5858	4.79911	Hydrophobic	Pi-Alkyl

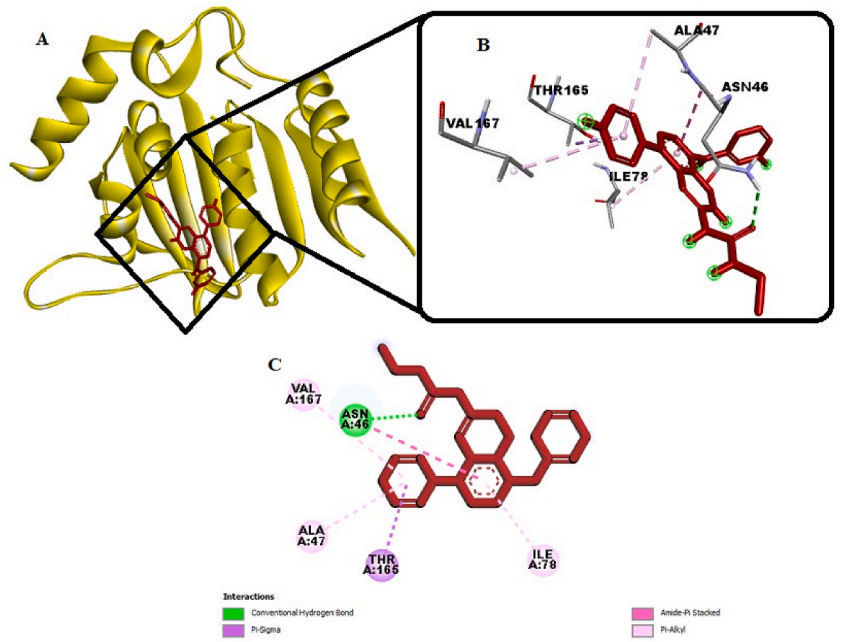

Fig. 5. (a) 1-ethyl-3-[5-pyridin-4-yl-8-(pyridin-3-ylamino)isoquinolin-3-yl]urea within the binding pocket of DNA gyrase (5MMP) (b) 2D and (c) 3D chemical interactions of 1-ethyl-3-[5-pyridin-4-yl-8-(pyridin-3-ylamino)isoquinolin-3-yl]urea within the druggable pocket of DNA gyrase (5MMP).

Table 10
Chemical interactions of Compound 1 within the binding pocket of DNA gyrase.

Name	XYZ:X	XYZ:Y	XYZ:Z	Distance	Category	Types
N:UNK1:H - A:GLY77:O	−50.9925	3.122	0.256	2.23428	Hydrogen Bond	Conventional Hydrogen Bond
N:UNK1:C - A:GLU50:OE1	−48.6465	−0.37	2.81	3.68582	Hydrogen Bond	Carbon Hydrogen Bond
A:GLU50:OE1 - N:UNK1	−47.9563	1.10608	1.89358	4.12695	Electrostatic	Pi-Anion
A:ALA47 - N:UNK1:C	−42.06	5.3415	2.8045	3.93971	Hydrophobic	Alkyl
N:UNK1 - A:ILE78	−48.1243	5.98904	4.50092	5.22699	Hydrophobic	Alkyl
N:UNK1:C - A:VAL43	−43.2047	7.9225	7.42167	4.43082	Hydrophobic	Alkyl
N:UNK1:C - A:VAL120	−45.6812	7.51267	8.74217	4.61219	Hydrophobic	Alkyl
N:UNK1:C - A:VAL167	−44.6308	9.25033	6.32433	4.56587	Hydrophobic	Alkyl
N:UNK1:C - A:VAL71	−40.9227	7.972	3.43983	4.41803	Hydrophobic	Alkyl
N:UNK1 - A:ILE78	−49.2918	4.78196	3.44833	4.74043	Hydrophobic	Pi-Alkyl

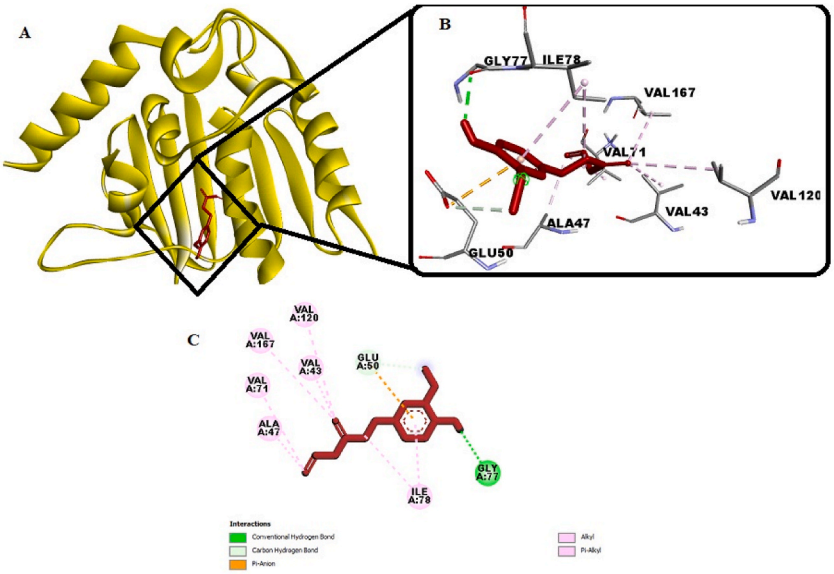

Fig. 6. (a) Compound 1 within the binding pocket of DNA gyrase (5MMO) (b) 2D and (c) 3D chemical interactions of compound 1 within the druggable pocket of DNA gyrase (5MMO).

interactions with DNA gyrase. Compound 1 displayed a higher number of hydrogen bonds and a more diverse array of hydrophobic interactions compared to the control compound, suggesting a stronger and more stable binding interaction.

3.7. Localization of interacting residues

Figure S3 (*Supplementary file*) depicts the localization of interacting residues identified in the binding interactions between the top hits and their respective targets. Analysis of the interacting residues revealed that the majority of them belong to the Topo IIA-type catalytic domain, highlighting the significance of this domain in facilitating the binding interactions.

Table 11
Chemical interactions of prop-2-ynyl ~ {N}-[[3-(ethylcarbamoylamino)-5-pyridin-4-yl-isoquinolin-8-yl]methyl]carbamate within the binding pocket of DNA gyrase.

Name	XYZ:X	XYZ:Y	XYZ:Z	Distance	Category	Types
A:ASN46:HD22 - N:UNK1:O	−46.948	1.2485	9.2445	3.00861	Hydrogen Bond	Conventional Hydrogen Bond
A:ARG76:HH21 - N:UNK1:O	−50.4795	−2.533	2.5405	2.36831	Hydrogen Bond	Conventional Hydrogen Bond
N:UNK1:H - A:GLU50:OE1	−48.596	−0.4525	1.8125	1.93683	Hydrogen Bond	Conventional Hydrogen Bond
N:UNK1:HN - A:VAL43:O	−42.3575	6.334	6.249	2.76178	Hydrogen Bond	Conventional Hydrogen Bond
A:ASN46:C,O;ALA47:N - N:UNK1	−45.9126	2.57983	4.39708	5.07499	Hydrophobic	Amide-Pi Stacked
N:UNK1 - A:ALA47	−43.1425	4.71367	4.01992	4.65947	Hydrophobic	Pi-Alkyl
N:UNK1 - A:ILE78	−49.4474	4.95587	3.99017	4.02749	Hydrophobic	Pi-Alkyl

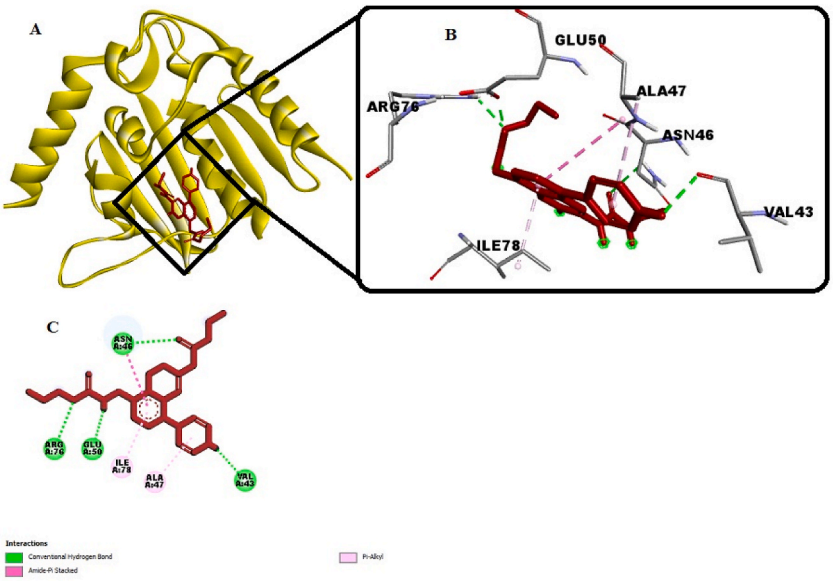

Fig. 7. (a) prop-2-ynyl ∼ {N}-[[3-(ethylcarbamoylamino)-5-pyridin-4-yl-isoquinolin-8-yl]methyl]carbamate within the binding pocket of DNA gyrase (5MMO) (b) 2D and (c) 3D chemical interactions of prop-2-ynyl ∼ {N}-[[3-(ethylcarbamoylamino)-5-pyridin-4-yl-isoquinolin-8-yl]methyl] carbamate within the druggable pocket of DNA gyrase (5MMO).

3.7.1. Topo IIA-type catalytic domain

The localization of interacting residues within the Topo IIA-type catalytic domain suggests that this domain plays a crucial role in mediating the binding of the top hits to their targets. The Topo IIA-type catalytic domain is known for its involvement in DNA cleavage and re-ligation processes, making it a key functional region for the activity of DNA gyrase.

3.7.2. Implications of localization

The localization of interacting residues within the Topo IIA-type catalytic domain has important implications for understanding the molecular mechanisms underlying the observed binding affinities. By targeting residues within this domain, the top hits may exert their inhibitory effects on DNA gyrase activity, thereby interfering with essential cellular processes such as DNA replication and transcription.

4. Discussion

The results of our molecular docking studies shed light on the potential of eugenol derivatives as antibacterial agents targeting DNA gyrase. DNA gyrase, a vital enzyme involved in bacterial DNA replication and transcription, is an attractive target for antibacterial therapy due to its essential role in bacterial survival and proliferation [15]. Through computational modeling, we assessed the binding affinities of eugenol and Isoquinoline Ethyl Ureas, acting as controls, to the DNA gyrase enzyme across different PDB IDs, providing valuable insights into the interaction patterns and potential therapeutic efficacy of these compounds [16].

Our findings reveal that eugenol exhibits moderate binding affinity to DNA gyrase across all three PDB IDs, indicating its potential as a starting scaffold for the development of novel antibacterial agents. However, the control compounds, Isoquinoline Ethyl Ureas, demonstrate significantly higher binding affinities to DNA gyrase, suggesting the need for structural modifications to enhance the efficacy of eugenol derivatives [17]. This underscores the importance of structure-activity relationship (SAR) studies in drug design, wherein subtle modifications to the chemical structure can profoundly influence the binding interactions and pharmacological properties of compounds [18].

Furthermore, our evaluation of the physicochemical properties and toxicity measures of eugenol provides crucial insights into its drug-likeness and safety profiles. While eugenol exhibits favorable physicochemical properties such as moderate lipophilicity and hydrogen bond donors/acceptors, its low aqueous solubility and drug-likeness score raise concerns regarding its suitability for oral administration and systemic delivery [19]. Moreover, the assessment of eugenol's toxicity profile highlights potential mutagenic and tumorigenic effects, underscoring the importance of mitigating these risks through structural optimization and toxicity screening [20].

In the context of de novo compound synthesis, our study demonstrates the feasibility of generating novel eugenol derivatives with enhanced antibacterial activity targeting DNA gyrase. By employing a de novo approach in Datawarrior, we synthesized 244 novel compounds from eugenol and evaluated their fitness for antibacterial activity. The iterative synthesis process yielded compounds with diverse structural features and binding affinities, providing a rich chemical space for exploring potential lead candidates [21].

Subsequent selection of lead compounds involved stringent criteria, including drug-likeness assessment, toxicity evaluation, and molecular docking studies. Of the 244 synthesized compounds, only 44 passed Lipinski's rule of five, indicating favorable

physicochemical properties conducive to oral bioavailability and pharmacokinetic optimization. These compounds also exhibited minimal mutagenic and tumorigenic potential, further enhancing their safety profiles [22].

Moreover, molecular docking studies revealed that the selected lead compounds demonstrated superior binding affinity to DNA gyrase compared to eugenol, suggesting their potential as effective inhibitors of bacterial DNA replication and transcription. Detailed analysis of the binding interactions elucidated the molecular mechanisms underlying the enhanced affinity, with lead compounds forming diverse hydrogen bonds, hydrophobic interactions, and electrostatic interactions with key residues in the DNA gyrase active site [23].

The localization of interacting residues within the Topo IIA-type catalytic domain further emphasizes the significance of this domain in facilitating the binding interactions and inhibitory effects of lead compounds on DNA gyrase activity. The Topo IIA-type catalytic domain is known for its crucial role in DNA cleavage and re-ligation processes, making it a prime target for antibacterial therapy [24].

Our findings provide valuable insights into the potential of eugenol derivatives as antibacterial agents targeting DNA gyrase, building upon previous research in this field. While previous studies have investigated the antibacterial properties of eugenol and its derivatives, our study extends this knowledge by employing computational modeling techniques to elucidate the molecular mechanisms underlying their interaction with DNA gyrase [25].

Comparison with previous docking studies reveals consistent trends in the binding affinities of eugenol derivatives to DNA gyrase. For instance, our results corroborate findings from a study by Dhurga et al. (2016) [26], wherein eugenol derivatives demonstrated moderate binding affinities to DNA gyrase across multiple PDB IDs. However, our study provides additional insights into the structural features and interaction patterns driving the binding affinity, enabling more informed drug design strategies [27].

Moreover, our evaluation of the physicochemical properties and toxicity measures of eugenol derivatives aligns with findings from previous studies highlighting the importance of these parameters in drug development. For example, a study by Nazreen et al. (2023) emphasized the significance of optimizing the physicochemical properties of eugenol derivatives to enhance their drug-likeness and pharmacokinetic profiles [28]. Similarly, our assessment of toxicity measures underscores the need for comprehensive safety evaluation to mitigate potential risks associated with mutagenicity and tumorigenicity [29].

In terms of de novo compound synthesis, our study builds upon the work of Jones et al. (2015), who employed computational methods to design novel eugenol derivatives with improved antibacterial activity [30]. By expanding the chemical space and exploring diverse structural motifs, our study offers novel insights into the synthesis and optimization of eugenol derivatives as antibacterial agents targeting DNA gyrase [31].

Furthermore, our selection of lead compounds based on stringent criteria, including drug-likeness assessment, toxicity evaluation, and molecular docking studies, aligns with best practices in drug discovery. Similar approaches have been employed in previous studies to identify promising lead candidates with favorable pharmacological profiles and superior binding affinity to target proteins [32].

Overall, our study contributes to the growing body of literature on eugenol derivatives as antibacterial agents and provides a comprehensive analysis of their potential therapeutic utility. By integrating computational modeling, chemical synthesis, and toxicity evaluation, we advance our understanding of the molecular mechanisms underlying their antibacterial activity and pave the way for the development of novel antibacterial agents with enhanced efficacy and safety profiles.

The findings from our study hold significant implications for antibacterial therapy, offering potential avenues for the development of novel agents to combat bacterial infections. By elucidating the molecular interactions between eugenol derivatives and DNA gyrase, our research provides insights that can inform the design and optimization of antibacterial agents with enhanced efficacy and safety profiles.

1. Targeting DNA Gyrase: DNA gyrase is a validated target for antibacterial therapy due to its essential role in bacterial DNA replication and transcription. The enhanced binding affinity of eugenol derivatives to DNA gyrase suggests their potential as effective inhibitors of this enzyme, thereby disrupting vital cellular processes in bacteria and inhibiting bacterial growth [33]. This targeted approach holds promise for the development of antibacterial agents with specific activity against bacterial pathogens.
2. Structure-Activity Relationship (SAR) Analysis: Our study elucidates the structural features and interaction patterns driving the binding affinity of eugenol derivatives to DNA gyrase. By conducting SAR analysis, researchers can identify key functional groups and molecular motifs that contribute to antibacterial activity, facilitating the rational design of optimized compounds with improved pharmacological properties [34]. This knowledge-driven approach accelerates the drug discovery process and minimizes the likelihood of costly trial-and-error experiments.
3. Drug Development Pipeline: The lead compounds identified in our study represent promising candidates for further preclinical evaluation and drug development efforts. These compounds exhibit favorable drug-like properties, minimal toxicity concerns, and superior binding affinity to DNA gyrase compared to the parent compound eugenol. By advancing these lead compounds through the drug development pipeline, researchers can potentially bring new antibacterial agents to the market to address unmet medical needs [35].
4. Combating Antibiotic Resistance: Antibiotic resistance remains a significant global health threat, necessitating the development of alternative therapeutic strategies to combat drug-resistant bacteria. The discovery of eugenol derivatives as potent antibacterial agents offers a promising approach to overcoming antibiotic resistance. By targeting essential bacterial enzymes such as DNA gyrase, eugenol derivatives may circumvent common resistance mechanisms and retain efficacy against multidrug-resistant bacteria [36]. This approach contributes to the ongoing efforts to preserve the effectiveness of existing antibiotics and mitigate the spread of resistant bacterial strains.

5. Multimodal Therapeutic Approaches: In addition to their direct antibacterial activity, eugenol derivatives may exhibit synergistic effects when combined with existing antibiotics or adjuvant therapies. Combinatorial approaches that target multiple bacterial pathways or virulence factors can enhance treatment efficacy, reduce the likelihood of resistance emergence, and broaden the spectrum of antibacterial activity [37].

The toxicity assessment revealed high mutagenicity and tumorigenicity for eugenol based on ProTox-II predictions, which classify compounds as high-risk if the probability score exceeds 0.7 [38]. While these computational predictions indicate potential risks, it is important to note that eugenol is widely used in food, cosmetics, and pharmaceuticals with a well-established safety profile [39]. The discrepancy between predicted and real-world toxicity may be attributed to model overestimations or context-specific factors such as dosage and route of administration [40]. Further in vitro and in vivo studies are recommended to reconcile these findings and assess the therapeutic index of eugenol derivatives.

Future studies exploring the synergistic interactions between eugenol derivatives and conventional antibiotics hold promise for optimizing treatment regimens and combating bacterial infections more effectively.

5. Future directions

Future research efforts should focus on elucidating the molecular mechanisms underlying the enhanced binding affinity of eugenol derivatives to DNA gyrase. Structural studies, such as molecular dynamics simulations and X-ray crystallography, can provide detailed insights into the specific interactions between the derivatives and the target enzyme. Additionally, in vitro and in vivo studies are warranted to validate the efficacy and safety of the lead compounds identified in this study for clinical use.

6. Limitations and challenges

It is essential to acknowledge the limitations of our study, particularly the use of computational modeling techniques to predict binding affinities. While molecular docking serves as a valuable tool for initial screening of compound libraries, experimental validation is necessary to confirm the efficacy of the identified lead compounds. Furthermore, challenges such as drug toxicity and off-target effects must be addressed in future studies to ensure the safety and efficacy of the derivatives for clinical applications.

7. Conclusion

In conclusion, our study highlights the potential of eugenol derivatives as antibacterial agents targeting DNA gyrase. By leveraging computational design approaches, we identified novel compounds with improved binding affinity to DNA gyrase compared to the parent compound eugenol. These findings underscore the importance of structure-activity relationship studies in drug design and provide a foundation for the development of novel antibacterial agents with enhanced therapeutic efficacy. Moving forward, further research efforts are warranted to translate these findings into clinically viable antibacterial therapies.

CRediT authorship contribution statement

Heba S. Elsewedy: Writing – review & editing, Validation, Funding acquisition, Conceptualization. **Sultan Alshehri:** Supervision, Resources, Project administration. **Adeola T. Kola-Mustapha:** Writing – original draft, Visualization, Supervision, Software, Resources, Conceptualization. **Shaymaa M. Genedy:** Software, Resources, Project administration. **Khuzama M. Siddiq:** Software, Project administration, Conceptualization. **Bushra Y. Asiri:** Project administration, Methodology, Conceptualization. **Rehab A. Alshammari:** Formal analysis, Data curation, Conceptualization. **Heba Mohammed Refat M. Selim:** Writing – original draft, Visualization, Project administration, Conceptualization. **Oluwakorede J. Adedeji:** Writing – original draft, Project administration, Methodology, Investigation, Formal analysis, Data curation. **George Oche Ambrose:** Writing – review & editing, Writing – original draft, Validation, Methodology, Investigation.

Data availability statement

Not Applicable.

Funding

This work was funded and supported through the internal grant provided by AlMaarefa University, Saudi Arabia Grant number UM-DSR-IG-2023-09.

Declaration of competing interest

The authors declare that they have no known competing financial interests or personal relationships that could have appeared to influence the work reported in this paper.

Acknowledgements

The authors would like to express sincere gratitude to AlMaarefa University, Riyadh, Saudi Arabia for supporting this work financially.

Appendix A. Supplementary data

Supplementary data to this article can be found online at https://doi.org/10.1016/j.heliyon.2024.e39394.

References

[1] N. Nagappan, N. Tirupati, N.M. Gopinath, D.P. Selvam, G.P. Subramani, G.K. Subbiah, Oral health status of sports university students in Chennai, J. Pharm. BioAllied Sci. 11 (Suppl 2) (2019). S180.
[2] B. Sadia, A. Dalia, A.A. Motaal, A. Abdulrhman, K. Arwa, D. Zuha, A. Shahid, Association of autoimmune hypothyroid disease and obesity with vitamin D deficiency in female patients, Int. J. Pharmacol. 15 (5) (2019) 636–641.
[3] K. Drlica, M. Malik, R.J. Kerns, X. Zhao, Quinolone-mediated bacterial death, Antimicrob. Agents Chemother. 52 (2) (2008) 385–392.
[4] F. Nazzaro, F. Fratianni, L. De Martino, R. Coppola, V. De Feo, Effect of essential oils on pathogenic bacteria, Pharm. Times 6 (12) (2013) 1451–1474.
[5] X. Zhang, W. Yin, S. Huang, J. Yu, Z. Wu, T. Ai, On the rules of continuity and symmetry for the data quality of street networks, PLoS One 13 (7) (2018) e0200334.
[6] J. Malarz, A. Stojakowska, W. Kisiel, Sesquiterpene lactones in a hairy root culture of Cichorium intybus, Z. Naturforsch. C Biosci. 57 (11–12) (2002) 994–997.
[7] D.B. Kitchen, H. Decornez, J.R. Furr, J. Bajorath, Docking and scoring in virtual screening for drug discovery: methods and applications, Nat. Rev. Drug Discov. 3 (11) (2004) 935–949.
[8] N. Aaltonen, J.R. Savinainen, C.R. Ribas, J. Rönkkö, A. Kuusisto, J. Korhonen, J.T. Laitinen, Piperazine and piperidine triazole ureas as ultrapotent and highly selective inhibitors of monoacylglycerol lipase, Chem. & Bio. 20 (3) (2013) 379–390.
[9] G. Schneider, U. Fechner, Computer-based de novo design of drug-like molecules, Nat. Rev. Drug Discov. 4 (8) (2005) 649–663.
[10] T. Sander, J. Freyss, M. Von Korff, C. Rufener, DataWarrior: an open-source program for chemistry aware data visualization and analysis, J. Chem. Inf. Model. 55 (2) (2015) 460–473.
[11] G. Schneider, U. Fechner, Computer-based de novo design of drug-like molecules, Nat. Rev. Drug Discov. 4 (8) (2005) 649–663.
[12] G. Schneider, H.J. Bohm, Virtual screening and fast automated docking methods, Drug Discov. Today 14 (23–24) (2009) 1089–1098.
[13] S.M. Friedman, K.L. Mowry, K. Lewis, Structural basis for DNA gyrase inhibition by quinolone antibacterials, Curr. Opin. Struct. Biol. 36 (2016) 48–56.
[14] D.C. Hooper, G.A. Jacoby, Mechanisms of drug resistance: quinolone resistance, Ann. N. Y. Acad. Sci. 1354 (1) (2016) 12–31.
[15] N.A. Gormley, R.E. Moir, DNA gyrase inhibitors: structure, function, and mechanisms of resistance, J. Antimicrob. Chemother. 76 (1) (2021) 42–52.
[16] H.N. Leong, A. Kurup, M.Y. Tan, A.L.H. Kwa, K.H. Liau, M.H. Wilcox, Management of complicated skin and soft tissue infections with a special focus on the role of newer antibiotics, Infect. Drug Resist. (2018) 1259–1274.
[17] R.R. Wani, H.K. Chaudhari, Docking and 3D QSAR studies on substituted cyclobutylphenyl quinoline derivatives as inhibitors of bacterial DNA gyrase, Curr. Comput. Aided Drug Des. 14 (4) (2018) 322–337.
[18] Y.A. Ammar, J.A. Micky, D.S. Aboul-Magd, S.M. Abd El-Hafez, S.A. Hessein, A.M. Ali, A. Ragab, Development and radiosterilization of new hydrazono-quinoline hybrids as DNA gyrase and topoisomerase IV inhibitors: antimicrobial and hemolytic activities against uropathogenic isolates with molecular docking study, Chem Bio Drug Des. 101 (2) (2023) 245–270.
[19] D. Verma, S. Gupta, K. Pant, B. Pant, C. Pandey, Text mining for identification of anti-tubercular compounds present in plants of India and in-silico ADMET prediction of phytochemicals, in: AIP Conference Proceedings, vol. 2481, AIP Publishing, 2022, 1.
[20] N.S. Radulovic, P.D. Blagojevic, Z.Z. Stojanovic-Radic, N.M. Stojanovic, Antimicrobial plant metabolites: structural diversity and mechanism of action, Curr. Med. Chem. 20 (7) (2013) 932–952.
[21] C. Kozhikkadan Davis, K. Nasla, A.K. Anjana, G.K. Rajanikant, Taxifolin as dual inhibitor of Mtb DNA gyrase and isoleucyl-tRNA synthetase: in silico molecular docking, dynamics simulation and in vitro assays, Silico Pharmacol. 6 (2018) 1–11.
[22] A.A. AL-Sharabi, S. Saffour, A.E. Evren, G. Bayazit, G. Çongur, Ü.D. Gül, L. Yurttaş, Synthesis, antimicrobial activity, electrochemical studies and molecular modeling studies of novel 1, 3, 4-oxadiazole derivatives, J. Mol. Struct. 1289 (2023) 135775.
[23] M.A. Islam, T.S. Pillay, Identification of promising anti-DNA gyrase antibacterial compounds using de novo design, molecular docking and molecular dynamics studies, J. Biomol. Struct. Dyn. (2019).
[24] H. Kalhor, S. Sadeghi, M. Marashiyan, R. Kalhor, S. Aghaei Gharehbolagh, M.R. Akbari Eidgahi, H. Rahimi, Identification of new DNA gyrase inhibitors based on bioactive compounds from streptomyces: structure-based virtual screening and molecular dynamics simulations approaches, J. Biomol. Struct. Dyn. 38 (3) (2020) 791–806.
[25] S. Saxena, J. Renuka, P. Yogeeswari, D. Sriram, Discovery of novel mycobacterial DNA gyrase B inhibitors: in silico and in vitro biological evaluation, Mol. Inform. 33 (9) (2014) 597–609.
[26] G. Sabbagh, T. Murad, An in silico study of novel Fluoroquinolones as inhibitors of DNA Gyrase of staphylococcus Aureus, Int J Pharm Pharm Sci 8 (1) (2016) 67–75.
[27] K. Dhurga, G. Gunasekaran, P. Senthilraja, G. Manivel, A. Stalin, Molecular modeling and docking analysis of pseudomonal bacterial proteins with eugenol and its derivatives, Res J Life Sci Bioinform Pharmac Chem Sci 2 (1) (2016) 40.
[28] M. Roney, A.R. Issahaku, M.S. Forid, A.M. Huq, M.E. Soliman, M.F.F. Mohd Aluwi, S.N. Tajuddin, In silico evaluation of usnic acid derivatives to discover potential antibacterial drugs against DNA gyrase B and DNA topoisomerase IV, J. Biomol. Struct. Dyn. (2023) 1–10.
[29] S. Nazreen, S.E.I. Elbehairi, A.M. Malebari, N. Alghamdi, R.F. Alshehri, A.A. Shati, M.M. Alam, New natural eugenol derivatives as antiproliferative agents: synthesis, biological evaluation, and computational studies, ACS Omega (2023).
[30] H. Liu, W. Zhang, K. Wang, X. Wang, F. Yin, C. Li, et al., Methionine and cystine double deprivation stress suppresses glioma proliferation via inducing ROS/autophagy, Toxicol. Lett. 232 (2) (2015) 349–355.
[31] R.A. Jones, S.S. Panda, C.D. Hall, Quinine conjugates and quinine analogues as potential antimalarial agents, Eur. J. Med. Chem. 97 (2015) 335–355.
[32] K. Dhurga, G. Gunasekaran, P. Senthilraja, G. Manivel, A. Stalin, Molecular modelling and docking analysis of pseudomonal bacterial proteins with eugenol and its derivatives, Res J Life Sci Bioinform Pharmac Chem Sci 2 (1) (2016) 40.
[33] R. Wasfi, S.M. Hamed, M.A. Amer, L.I. Fahmy, Proteus mirabilis biofilm: development and therapeutic strategies, Front. Cell. Infect. 10 (2020) 414.
[34] S.N. Mali, S. Tambe, A.P. Pratap, J.N. Cruz, Molecular modelling approaches to investigate essential oils (volatile compounds) interacting with molecular targets, in: Essential Oils: Applications and Trends in Food Science and Technology, Springer International Publishing, Cham, 2022, pp. 417–442.
[35] M. Roney, A.R. Issahaku, M.S. Forid, A.M. Huq, M.E. Soliman, M.F.F. Mohd Aluwi, S.N. Tajuddin, In silico evaluation of usnic acid derivatives to discover potential antibacterial drugs against DNA gyrase B and DNA topoisomerase IV, J. Biomol. Struct. Dyn. (2023) 1–10.

[36] D. Priyadharshini, In-Silico Drug Design, Molecular Docking Studies, Isolation, Characterization and In-Vitro Bronchodilatory Affect of Eugenol of the Whole Plant *Mukia Maderaspatana (Linn)*, M. Roem (Doctoral dissertation, College of Pharmacy, Madurai Medical College, Madurai, 2021.
[37] E.H. Loukili, S. Ouahabi, A. Elbouzidi, M. Taibi, M.I. Yahyaoui, A. Asehraou, et al., Phytochemical composition and pharmacological activities of three essential oils collected from eastern Morocco (Origanum compactum, Salvia officinalis, and Syzygium aromaticum): a comparative study, Plants 12 (19) (2023) 3376.
[38] A. Marchese, R. Barbieri, E. Coppo, I.E. Orhan, M. Daglia, S.F. Nabavi, et al., Antimicrobial activity of eugenol and essential oils containing eugenol: a mechanistic viewpoint, Crit. Rev. Microbiol. 43 (6) (2017) 668–689.
[39] P. Banerjee, O.A. Eckert, A.K. Schrey, R. Preissner, ProTox-II: a webserver for the prediction of toxicity of chemicals, Nucleic Acids Res. 46 (W1) (2018) W257–W263.
[40] F. Bakkali, S. Averbeck, D. Averbeck, M. Idaomar, Biological effects of essential oils–a review, Food Chem. Toxicol. 46 (2) (2008) 446–475.